Electronic Supplementary Material (ESI) for Journal of Materials Chemistry A.
This journal is © The Royal Society of Chemistry 2024

Supporting Information

Disparity among cyclic alkyl carbonates associated with cathode electrolyte interphase at high voltage

Shuaishuai Chen[a], YiHan Tang, Zhaoxin Lu, Shun Wu,

Jiliang Wu*[, b], Zhenlian Chen*[, a], Deyu Wang*[, a]

a: Key Laboratory of Optoelectronic Chemical Materials and Devices, Ministry of Education, School of Optoelectronic Materials & Technology, Jianghan University, Wuhan 430056, China

b: Wuhan Zhongyuan Changjiang Technology Development Co. Ltd., Wuhan 430090, China

Dr. Jiliang Wu, jlwu@whu.edu.cn

Associate Prof. Zhenlian Chen, zhenlianchen@jhun.edu.cn

Prof. Deyu Wang, wangdeyu@jhun.edu.cn

Experimental sections

The several solvents and solutes used in this work were commercial materials, included ethylene carbonate (EC), fluoroethylene carbonate (FEC), propylene carbonate (PC), dimethyl carbonate (DMC)， methyl ethyl carbonate (EMC) and $LiPF_6$. The electrolytes with different proportions were prepared in an argon-filled glovebox (H_2O & O_2 contents < 1 ppm). EC: DMC: EMC / FEC: DMC: EMC / PC: DMC: EMC were mixing with volume ratio=1:1:1, $LiPF_6$ was selected as solute. The electrolytes were named EC-based, FEC-based, and PC-based, respectively. The electrolytes and their conductivity are shown in Figure S2&S3.

The measurements of the conductivity of the electrolytes were performed on DDS-307A conductivity meters with a titanium alloy electrode (K = 0.01). The linear sweep voltammetry (LSV) measurements were conducted on Solartron electrochemical station. The chemical compositions of CEI films were acquired from FTIR spectra (Bruker ALPHA).The surface morphology of $LiCoO_2$ was characterized by both Scanning Electron Microscopy (SEM Quanta 250, FEI) and Transmission Electron Microscopy (TEM, JEM2100, JEOL). The chemical compositions of the cathode interfacial layer were analyzed by XPS (AXIS Ultra, Kratos) with Al Kα line as an X-ray source. Binding energies were calibrated by using the carbon content (C1s = 284.8 eV). The chemical compositions of the cathode interfacial layer were analyzed by TOF-SIMS (TOF SIMS ION-TOF GmbH) with a mass resolution of over 5000. The mass spectrometry was equipped with a 30 kV Bi^+ analysis beam for depth profiling or high-resolution mapping analysis in high current mode or burst alignment mode. Depending on the secondary ion polarity, a 500 eV Cs^+ ion beam or a 1 keV O^{2+} ion beam was applied for the negative mode. The sputtering and analysis areas are 100 × 100 μm^2.

The electrochemical performance was achieved on the Land CT2001A multichannel battery cycler equipment by assembling CR2032 coin cell of $LiCoO_2$/Li. Li foils were used as the negative electrodes. The cathode electrode was prepared by a homogenous slurry which was consisted of 80 wt.% active cathode materials, 10 wt.% super P and 10 wt.% polyvinylidene fluoride (PVDF) binder, dispersing the solid powders in N-methyl pyrrolidone (NMP) solvent. After stirring for 5h, the as-prepared slurry was coated on aluminum (Al) foil. The electrode was dried at 120°C under vacuum and punched into circular discs with a diameter of 14 mm. The thickness of the Li foil was 200 μm,

and the amount of the electrolyte used in the coin cell was 70 μL.

Simulation Method

DFT calculations are carried out using the Damping Function in Dispersion Corrected[1] density functional theory (DFT) method as implemented in the Gaussian 16 suite of programs (Gaussian 16, Revision B.01, Frisch, M.J., Trucks, G.W., Schlegel, H.B., Scuseria, G.E., Robb, M.A., Cheeseman, J.R.; Scalmani, G.; Barone, V.; Petersson, G.A.; Nakatsuji, H.; Li, X.; Caricato, M.; Marenich, A.V.; Bloino, J., Janesko, B.G., Gomperts, R., Mennucci, B., Hratchian, H.P., Ortiz, J.V., Izmaylov, A.F., Sonnenberg, J.L., Williams-Young, D., Ding, F., Lipparini, F., Egidi, F., Goings, J., Peng, B., Petrone, A., Henderson, T., Ranasinghe, D., Zakrzewski, V.G., Gao, J., Rega, N., Zheng, G., Liang, W., Hada, M., Ehara, M., Toyota, K., Fukuda, R., Hasegawa, J., Ishida, M., Nakajima, T., Honda, Y., Kitao, O., Nakai, H., Vreven, T., Throssell, K., Montgomery Jr., J.A., Peralta, J.E., Ogliaro, F., Bearpark, M.J., Heyd, J.J., Brothers, E.N., Kudin, K.N., Staroverov, V.N., Keith, T.A., Kobayashi, R., Normand, J., Raghavachari, K., Rendell, A.P., Burant, J.C., Iyengar, S.S., Tomasi, J., Cossi, M., Millam, J.M., Klene, M., Adamo, C., Cammi, R., Ochterski, J.W., Martin, R.L., Morokuma, K., Farkas, O., Foresman, J.B., Fox, D.J. Gaussian, Inc., Wallingford CT (2016)) with the basis sets 6-311G+(d,p).[2, 3] For each transition state, intrinsic reaction coordinate (IRC) calculation is performed in both directions to connect these corresponding intermediates at the above level.

Figure S1. The molecular structure of the decomposition products and carbon chain number.

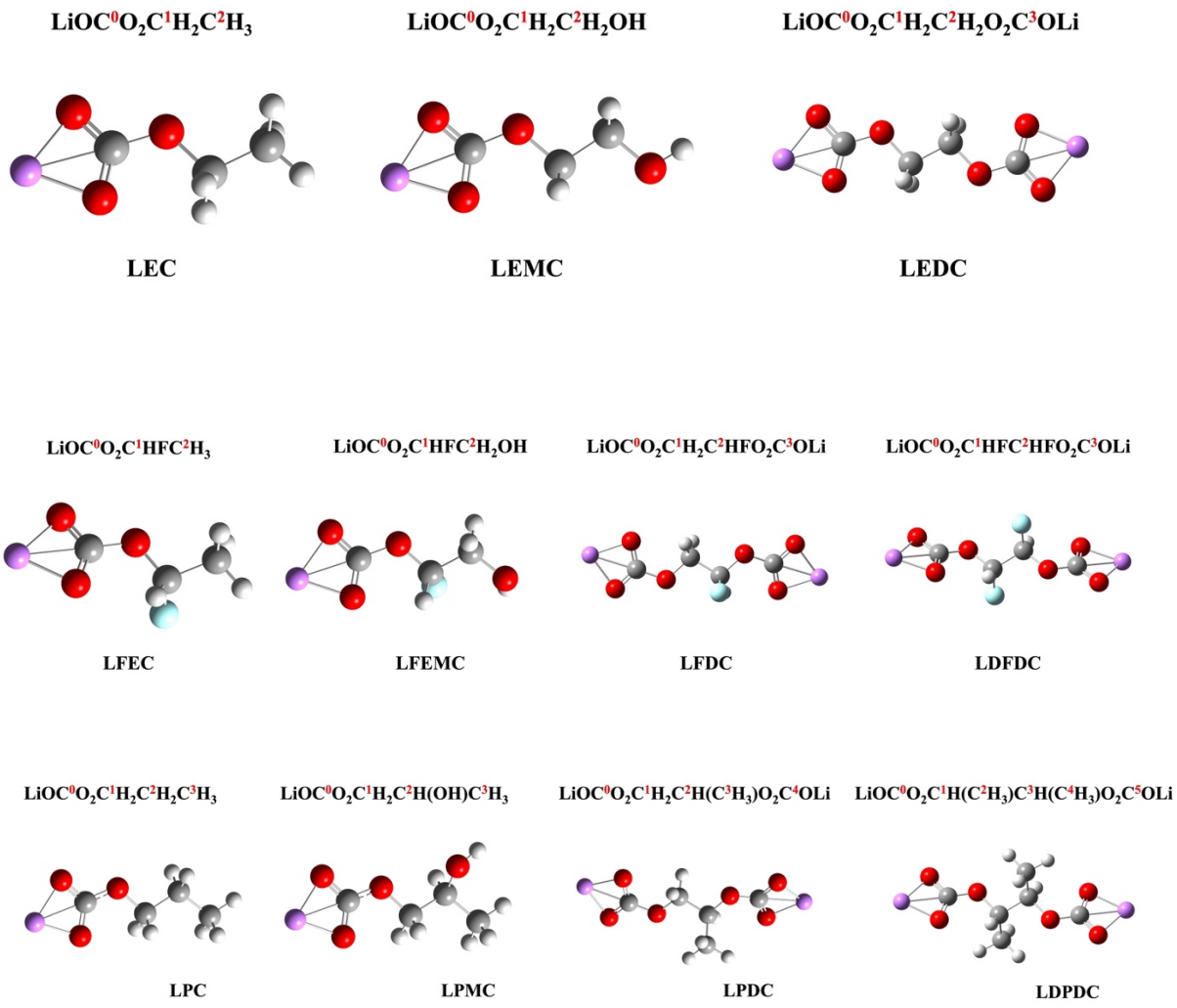

Figure S2. The photos of three electrolytes.

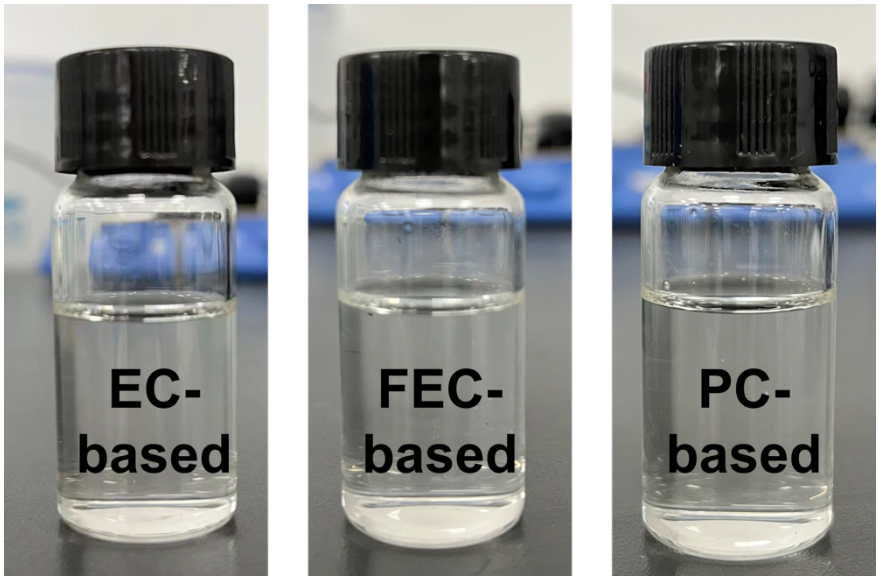

Figure S3. Conductivity of three electrolytes.

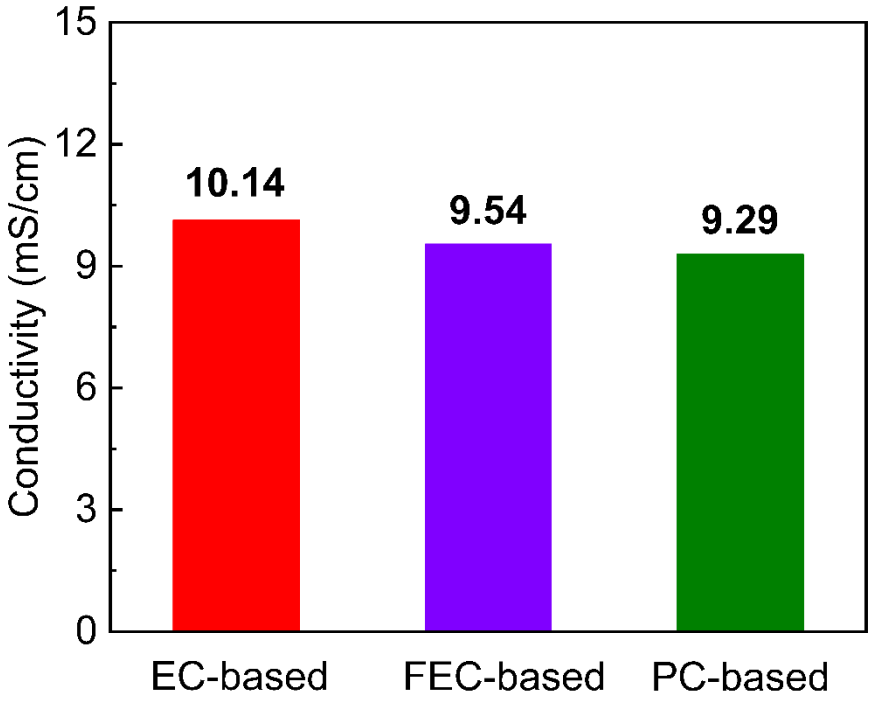

Figure S4. The test of constant-voltage polarization.

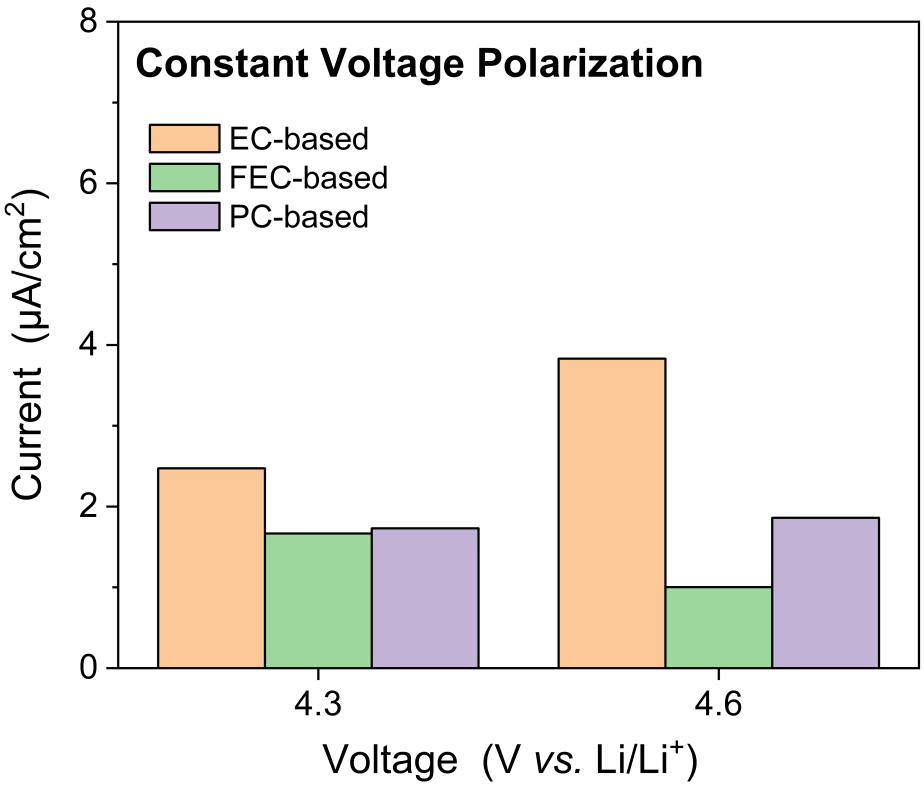

Figure S5. Electrochemical performance of Li/$LiCoO_2$ cells with different electrolytes at 2.8-4.3V/4.6 V (*vs.* Li/Li^+), the rate is 0.1 C in first cycle and 1 C in 300^{th} cycle.

The capacity radio of 300th/1st					
EC-4.3 V	FEC-4.3 V	PC-4.3 V	EC-4.6 V	FEC-4.6 V	PC-4.6 V
69.09%	79.88%	74.60%	7.71%	73.84%	66.05%

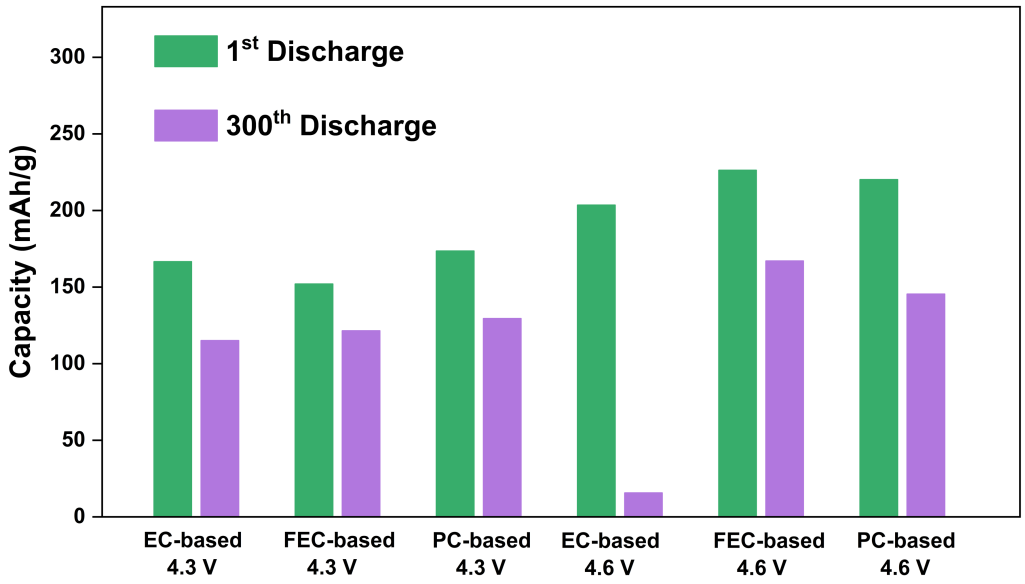

Figure S6. TOF-SIMS analysis of EC-based by negative mode with cut-off voltage of 4.3 V *vs.* Li/Li^+.

Depth profile curves of three different electrolytes.

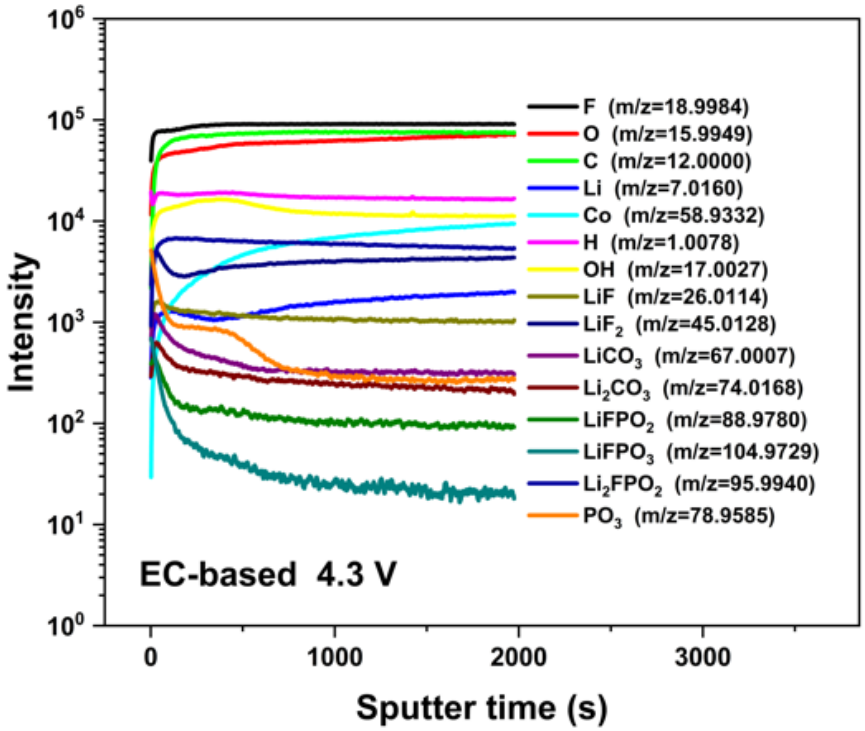

Figure S7. TOF-SIMS analysis of FEC-based by negative mode with cut-off voltage of 4.3 V *vs.* Li/Li^+.

Depth profile curves of all signal information.

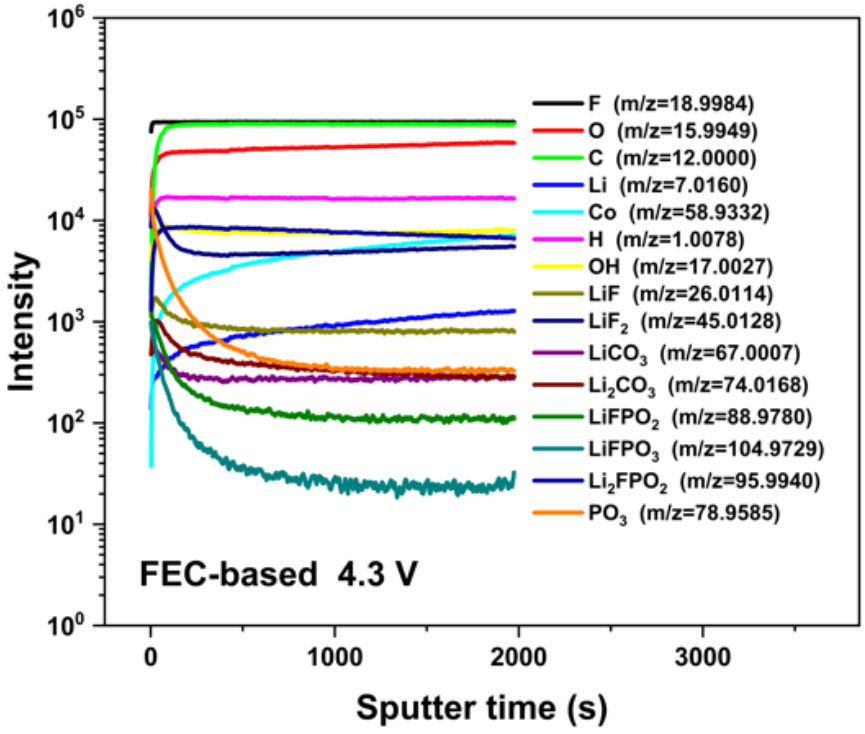

Figure S8. TOF-SIMS analysis of PC-based by negative mode with cut-off voltage of 4.3 V *vs.* Li/Li^+.

Depth profile curves of all signal information.

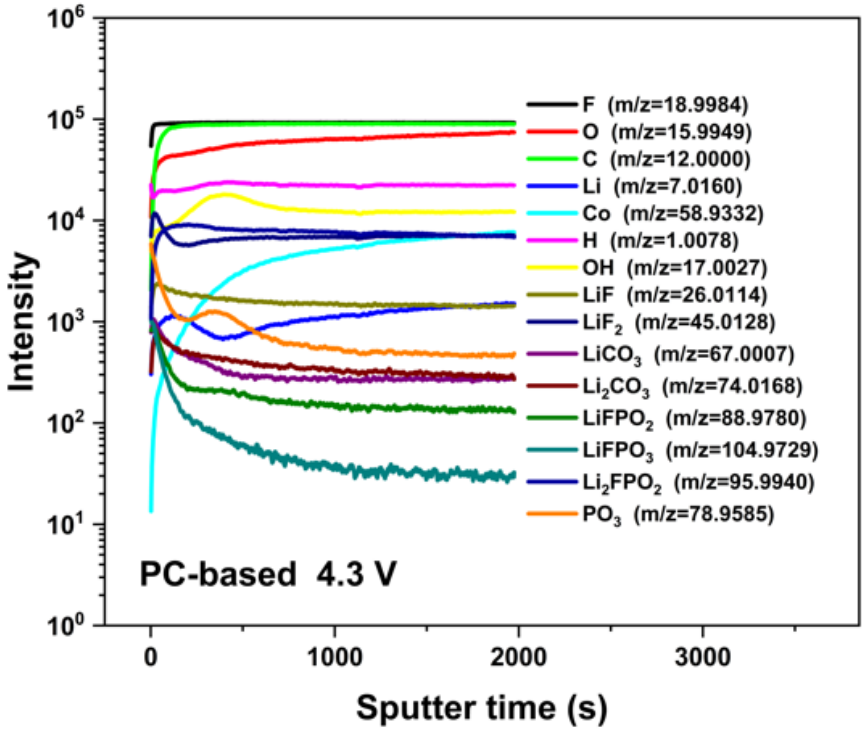

Figure S9. TOF-SIMS analysis by negative mode with cut-off voltage of 4.3V *vs.* Li/Li^+. Mass spectrum collected at sputter stage, (a) EC-based, (b) FEC-based, (c) PC-based.

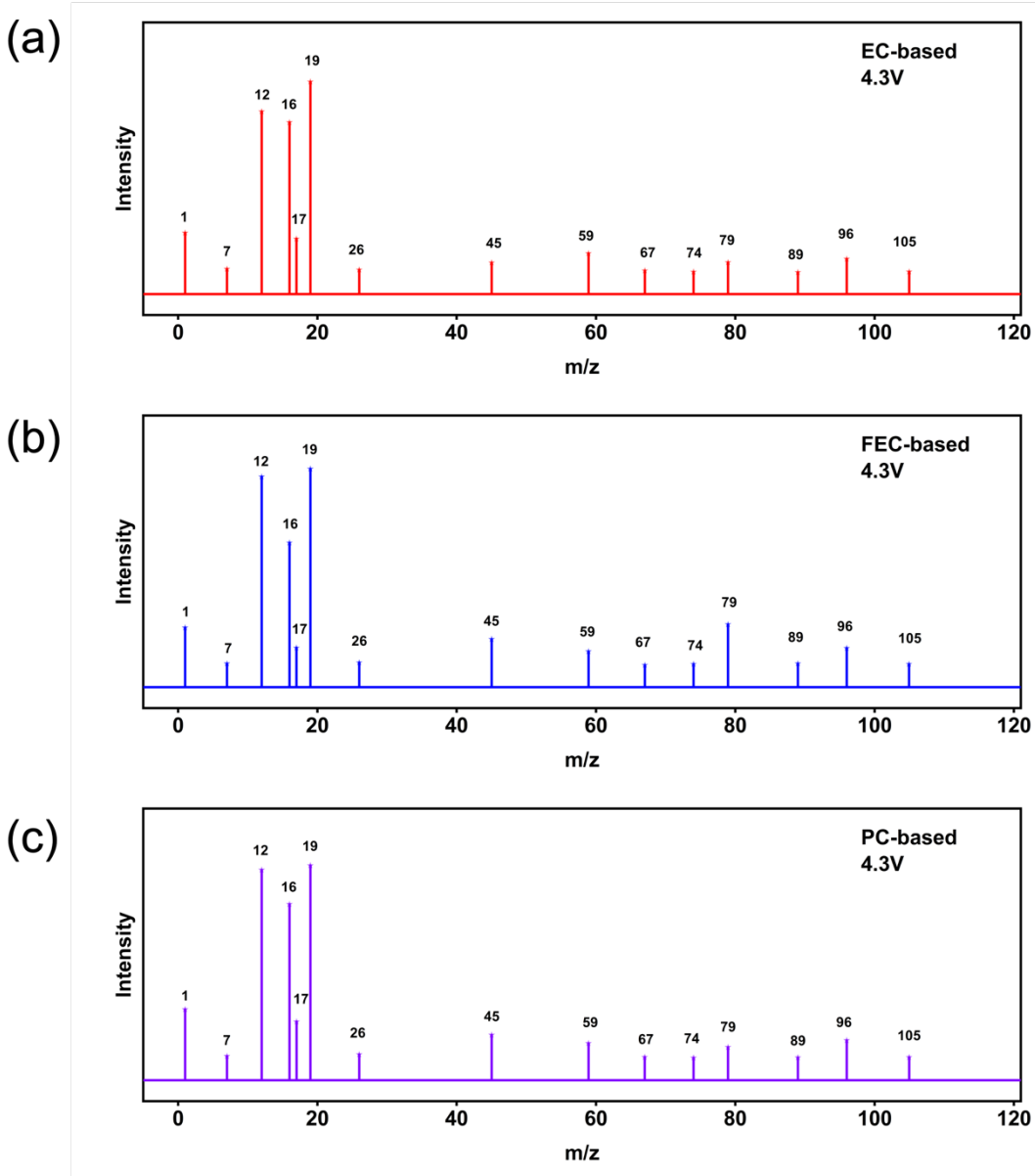

Figure S10. TOF-SIMS analysis of EC-based by negative mode with cut-off voltage of 4.6 V *vs.* Li/Li^+.

Depth profile curves of all signal information.

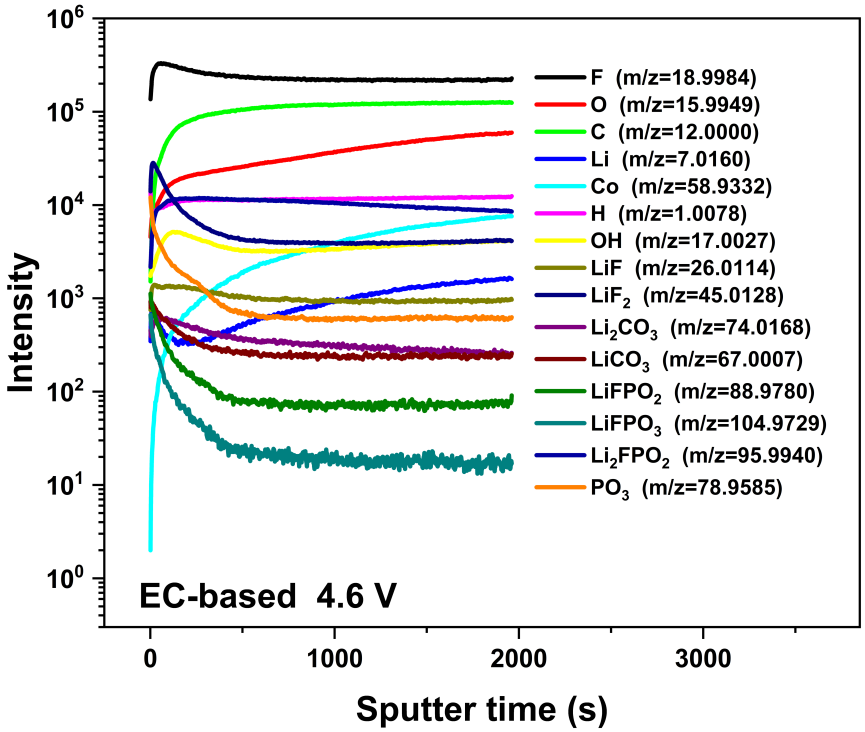

Figure S11. TOF-SIMS analysis of FEC-based by negative mode with cut-off voltage of 4.6 V *vs.* Li/Li^+.

Depth profile curves of all signal information.

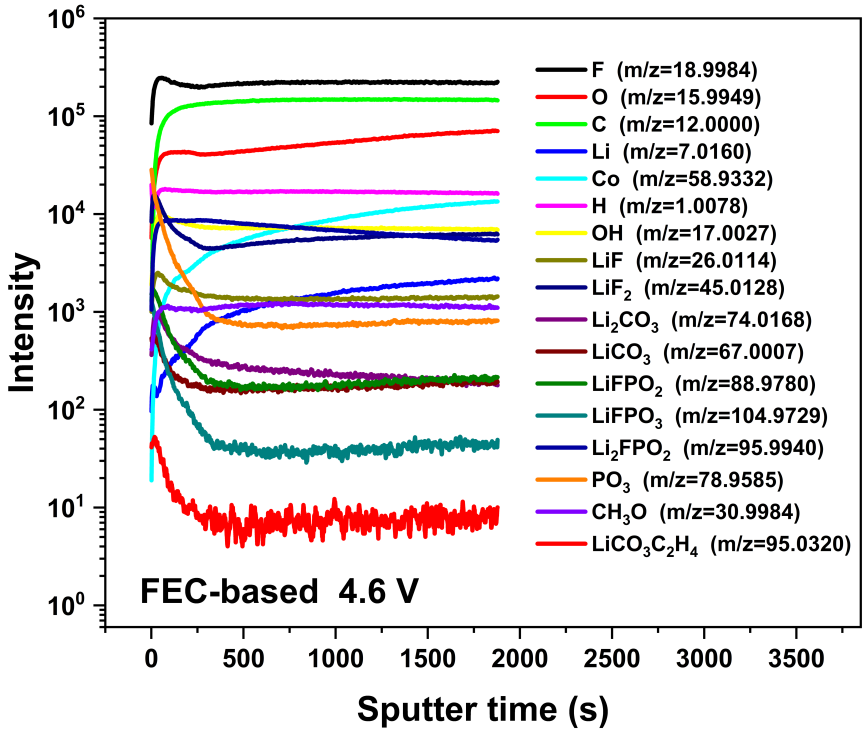

Figure S12. TOF-SIMS analysis of PC-based by negative mode with cut-off voltage of 4.6 V *vs.* Li/Li^+.

Depth profile curves of all signal information.

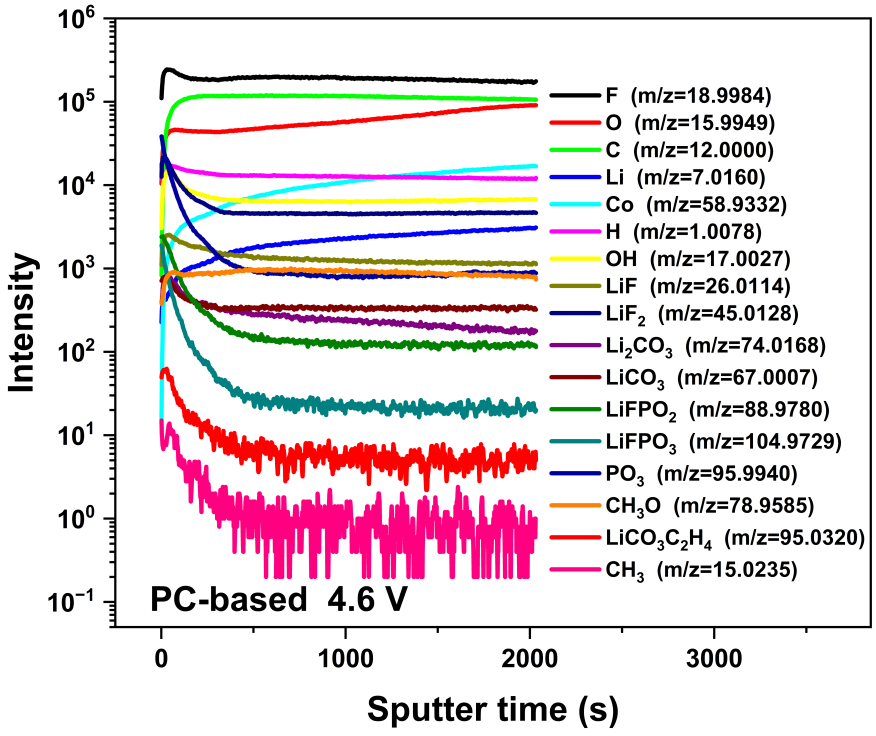

Figure S13. SEM images of $LiCoO_2$ electrodes uncycled and after 5 charge/discharge cycles in different electrolytes. (a) Fresh, (b) EC-based, (c) FEC-based, (d) PC-based.

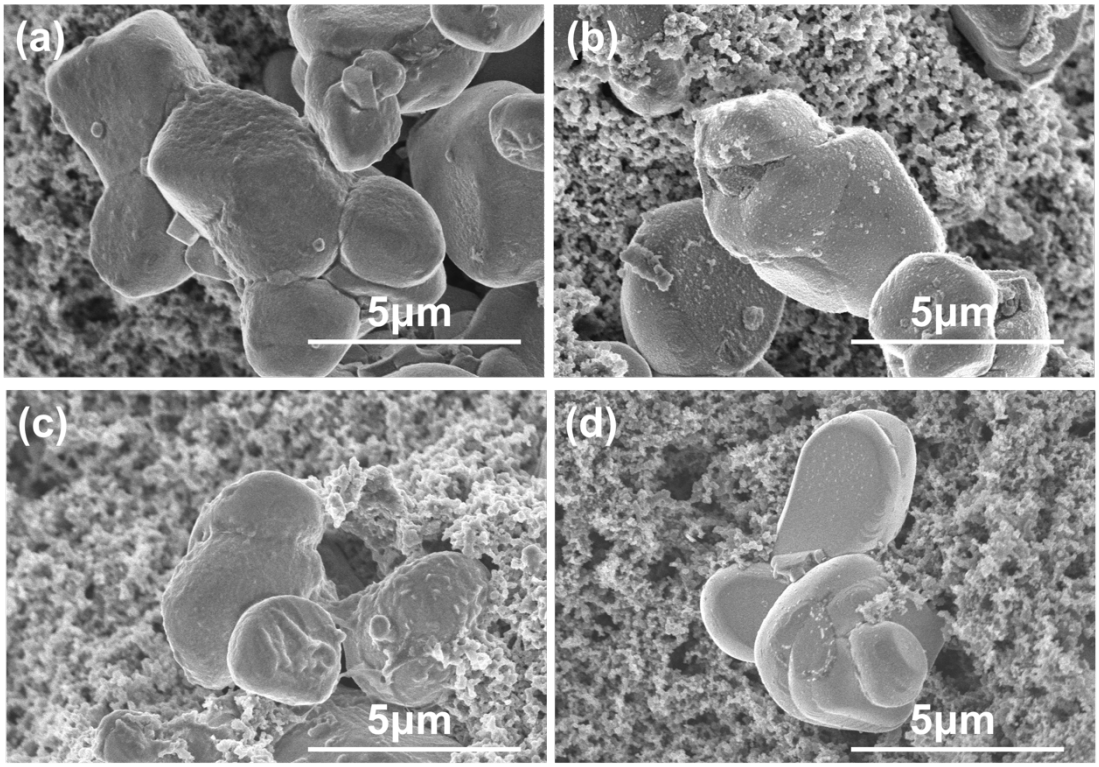

Figure S14. TEM images of $LiCoO_2$ electrode after 5 charge/discharge cycles with different electrolytes at 4.3 V *vs.* Li/Li^+. (a). EC-based, (b). FEC-based, (c). PC-based.

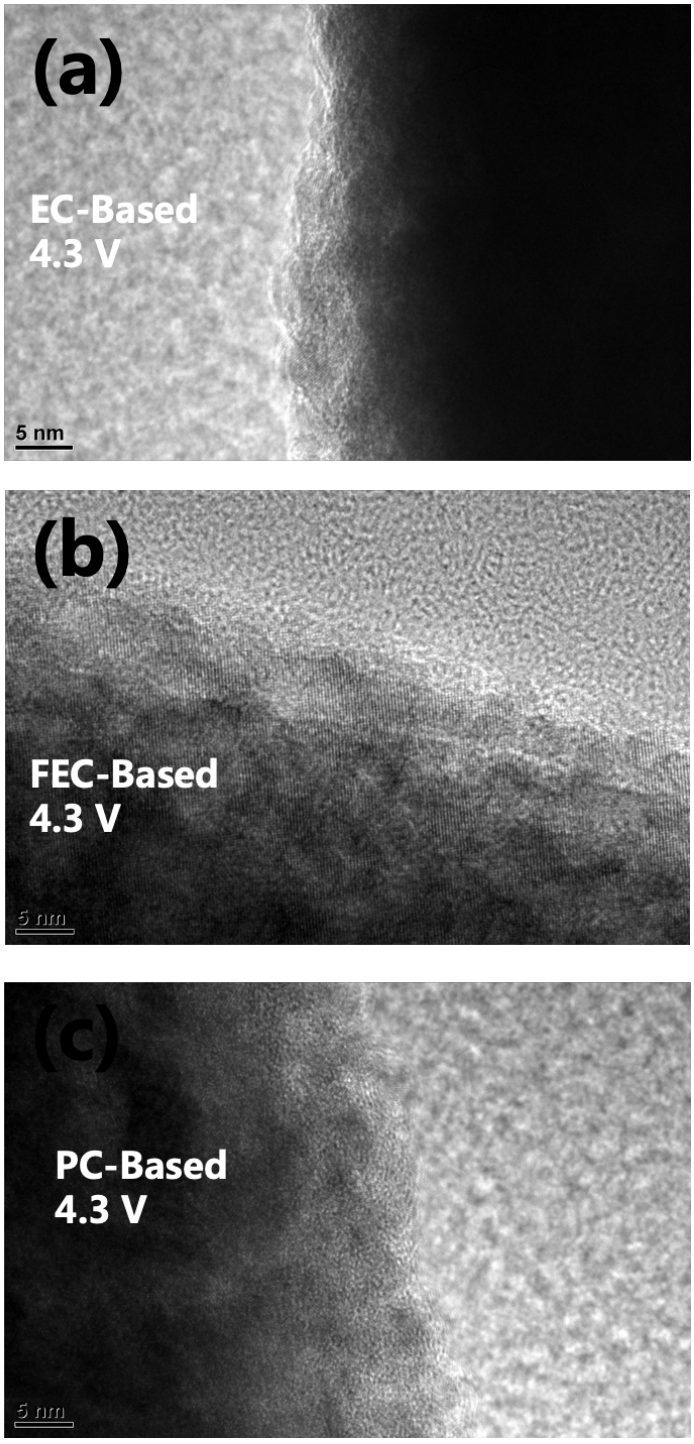

Figure S15. XPS spectra of Co 2p.

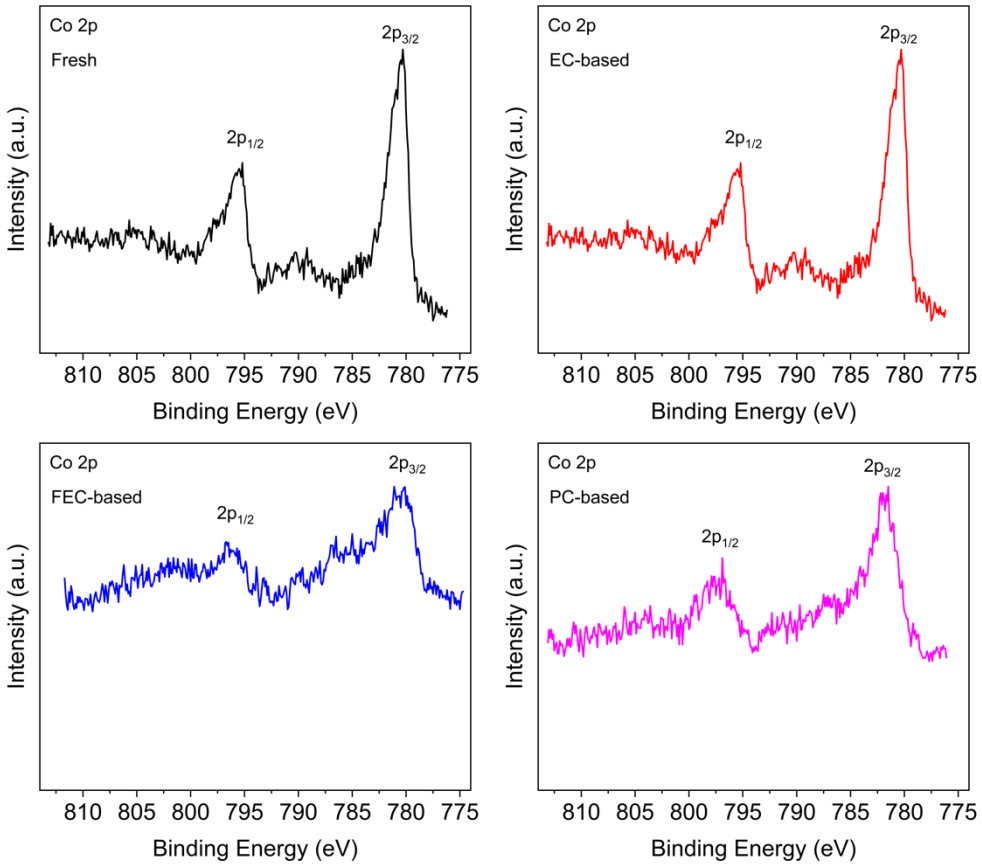

Table S1. The absolute values of calculated LUMO, HOMO and calculated value of ΔG_R, ΔG_O, ΔG_H for 11 possible side products.

Solvent	Name	LUMO	HOMO	ΔG_O	ΔG_{H-1}	ΔG_{H-2}	ΔG_{H-3}	ΔG_{H-O}
EC-based	LEC	-1.07	-7.32	9.04	3.72	4.05		
	LEMC	-1.10	-7.36	9.01	4.19	3.67		3.94
	LEDC	-1.06	-7.28	8.62	3.74	3.74		
FEC-based	LFEC	-1.20	-7.68	9.24	3.89	4.07		
	LFEMC	-1.31	-7.77	9.36	3.97	3.69		4.05
	LFDC	-1.18	-7.38	8.80	3.74	3.81		
	LDFDC	-1.20	-7.70	9.02	4.00	4.00		
PC-based	LPC	-1.07	-7.26	8.91	3.97	3.78	3.92	
	LPMC	-1.04	-7.23	8.48	3.74	3.51	4.08	3.75
	LPDC	-1.05	-7.24	8.56	3.79	3.78	3.92	
	LDPDC	-1.03	-7.21	8.48	3.79	3.99		

(The serial number of C carbon is shown in Figure S14. H-1 corresponds to H atom on C^1 atom, H-2 corresponds to H atom on C^2 atom, H-3 corresponds to H atom on C^3 atom, H-O corresponds to H atom on hydroxyl.)

Table S2. Decomposition products information.

Name	Short Name	Chemical Formula	Molecular Formula	Molecular Weight	m/z
Lithium ethyl carbonate	LEC	$C_3H_5LiO_3$	$LiOCO_2CH_2CH_3$	96.0100	96.0399
Lithium ethylene mono-carbonate	LEMC	$C_3H_5LiO_4$	$LiOCO_2CH_2CH_2OH$	112.0090	112.0348
Lithium ethylene di-carbonate	LEDC	$C_4H_4Li_2O_6$	$(CH_2CO_2OLi)_2$	161.9500	162.0328
Lithium fluoroethyl carbonate	LFEC	$C_3H_4FLiO_3$	$LiOCO_2CHFCH_3$	114.0004	114.0305
Lithium fluoroethylene mono-carbonate	LFEMC	$C_3H_4FLiO_4$	$LiOCO_2CHFCH_2OH$	129.9994	130.0254
Lithium fluoroethylene di-carbonate	LFDC	$C_4H_3FLi_2O_6$	$LiOCO_2C_2FH_3CO_2OLi$	179.9404	180.0234
Lithium di-fluoroethylene di-carbonate	LDFDC	$C_4H_2F_2Li_2O_6$	$(C_2FH_3CO_2OLi)_2$	197.9308	198.0140
Lithium propyl carbonate	LPC	$C_4H_7LiO_3$	$LiOCO_2CH_2CH_2CH_3$	110.0370	110.0555
Lithium propylene mono-carbonate	LPMC	$C_4H_7LiO_4$	$LiOCO_2CH_2CH(OH)CH_3$	126.0360	126.0504
Lithium propylene di-carbonate	LPDC	$C_5H_6Li_2O_6$	$LiOCO_2C_3H_6CO_2OLi$	175.9770	176.0484
Lithium di-propylene di-carbonate	LDPDC	$C_6H_8Li_2O_6$	$(C_2H_4CO_2OLi)_2$	190.0040	190.0641

Table S3. The molecular structural formula of solvent and decomposition products.

Solvent	Structural formula	Decomposition products			
EC	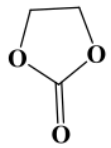	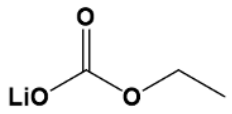 (LEC)	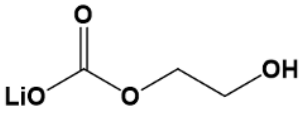 (LEMC)	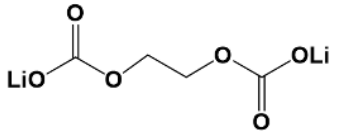 (LEDC)	
FEC	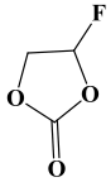	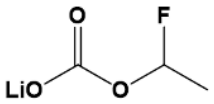 (LFEC)	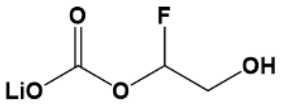 (LFEMC)	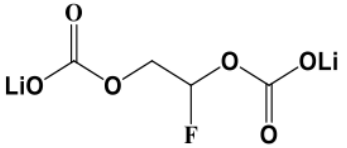 (LFDC)	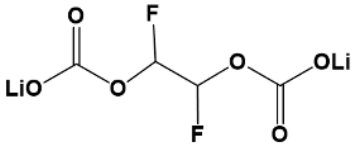 (LDFDC)
PC	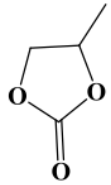	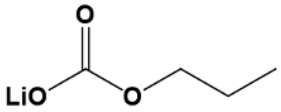 (LPC)	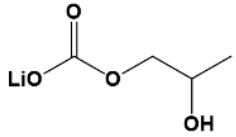 (LPMC)	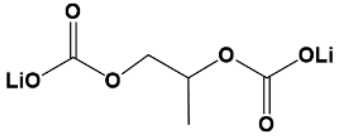 (LDPC)	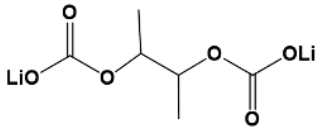 (LDPDC)

Table S4. Content percent (%) of element F in different bonds.

XPS Peak/(%)	C-F & $Li_xP_yFO_z$	LiF
EC-based	83.52	16.48
FEC-based	66.31	33.69
PC-based	79.03	21.97

References

(1) Grimme, S.; Ehrlich, S.; Goerigk, L. Effect of the damping function in dispersion corrected density functional theory. *J Comput Chem* **2011**, *32* (7), 1456-1465. DOI: 10.1002/jcc.21759.

(2) Weigend, F.; Ahlrichs, R. Balanced basis sets of split valence, triple zeta valence and quadruple zeta valence quality for H to Rn: Design and assessment of accuracy. *Phys Chem Chem Phys* **2005**, *7* (18), 3297-3305. DOI: 10.1039/b508541a.

(3) Weigend,F. Accurate Coulomb-fitting basis sets for H to Rn. *Phys Chem Chem Phys* **2006**, *8* (9), 1057-1065. DOI: 10.1039/b515623h.